


## RESEARCH ARTICLE OPEN ACCESS

# Innovation in CRC Research: Targeting SPACA6P-AS for Progression

Tianyi Ma<sup>1</sup>  | Yinghu Jin<sup>1</sup> | Song Wang<sup>2</sup> | Hanqing Hu<sup>1</sup> | Meng Wang<sup>3</sup> | Guoqing Yan<sup>1</sup> | Qingchao Tang<sup>1</sup> | Rui Huang<sup>1</sup> | Guiyu Wang<sup>1</sup>

<sup>1</sup>Department of Colorectal Surgery, the Second Affiliated Hospital of Harbin Medical University, Harbin, China | <sup>2</sup>Department of Colorectal Surgery, the First Affiliated Hospital, Zhejiang University School of Medicine, Hangzhou, China | <sup>3</sup>Department of Colorectal Surgery, Zhejiang Cancer Hospital (Affiliated Cancer Hospital of the Chinese Academy of Sciences), Hangzhou, China

**Correspondence:** Guiyu Wang ([guiyuwang@163.com](mailto:guiyuwang@163.com))

**Received:** 12 March 2024 | **Revised:** 27 September 2024 | **Accepted:** 16 October 2024

**Funding:** This research was partially funded by the Scientific Research Project of the Heilongjiang Provincial Health and Family Planning Commission (Grant No. 2018249), the Heilongjiang Provincial Higher Education Innovation Fund (Grant No. 31041210019), and the Second Affiliated Hospital of Harbin Medical University standardized training project for resident doctors (Grant No.2020020225).

**Keywords:** colorectal cancer | FAM167A | long noncoding RNA | miR-339-5p | prognosis | proliferation | SPACA6P-AS

## ABSTRACT

The purpose of this research was to provide light on the functional role that the long noncoding RNA SPACA6P-AS plays in the biology of colorectal cancer (CRC). The presence of elevated SPACA6P-AS expression in colorectal cancer tissues is linked to advanced stages of the disease as well as a decreased overall survival rate. It has been demonstrated through knockdown tests conducted on CRC cell lines that SPACA6P-AS stimulates cell growth in both in vitro and in vivo settings. By acting as a competing endogenous RNA, SPACA6P-AS is able to modulate the levels of miR-339-5p and promote the proliferation of colorectal cancer cells by way of the miR-339-5p/FAM167A/FAM167A signaling axis. Based on these findings, SPACA6P-AS is a promising candidate for both a prognostic marker and a therapeutic target in colorectal cancer.

## 1 | Introduction

Colorectal cancer (CRC) remains a critical global health issue, with its prevalence and associated mortality demonstrating a concerning upward trajectory each year [1, 2]. This trend persists despite significant advances in treatment options and surgical interventions. Recent years have seen the introduction of cutting-edge therapies like immunotherapy and enhanced surgical methods, notably total mesorectal excision [3, 4]. Yet, the high mortality rate linked to CRC, particularly in its advanced stages, underscores an urgent need for ongoing research and development of more effective treatment strategies. While patients with early-stage CRC can expect a 5-year survival rate of approximately 90%, those diagnosed at later stages (III and IV) face considerably lower survival rates, highlighting the critical importance of early detection and novel therapeutic approaches [5–7].

One area of promising research is the study of long noncoding RNAs (lncRNAs), which are RNA sequences longer than 200 nucleotides and do not code for proteins [8]. lncRNAs have been shown to play diverse roles in numerous cellular and biological processes, including but not limited to cellular differentiation, proliferation, and the development of various cancers [9–12]. Although initially considered as nonfunctional or “dark matter” in the genome, current research has shed light on the crucial roles that lncRNAs play in gene regulation and other key biological functions [13–15]. Their involvement is particularly noted in the context of cancer, where they are being explored as potential biomarkers and therapeutic targets. This exploration extends into the realm of oncology, where specific lncRNAs are increasingly recognized for their roles in tumor regulation. Notably, the lncRNA SPACA6P-AS, spanning 3962 nucleotides, has recently been identified as an oncogene in

This is an open access article under the terms of the [Creative Commons Attribution-NonCommercial](https://creativecommons.org/licenses/by-nc/4.0/) License, which permits use, distribution and reproduction in any medium, provided the original work is properly cited and is not used for commercial purposes.

© 2024 The Author(s). *Journal of Biochemical and Molecular Toxicology* published by Wiley Periodicals LLC.

hepatocellular carcinoma, drawing attention to its potential role in other cancer types, including CRC [16].

The oncogenic properties of SPACA6P-AS in hepatocellular carcinoma have been well-documented, but its involvement in CRC is not yet fully understood. The exploration of SPACA6P-AS in CRC is thus imperative, as it may offer new insights and opportunities for therapeutic intervention. In our study, we report the overexpression of lncRNA SPACA6P-AS in CRC tissues. Our investigations reveal that SPACA6P-AS may function as a competing endogenous RNA (ceRNA), engaging in molecular interactions with miR-339-5p. This interaction appears to influence the expression of FAM167A, a gene implicated in cancer development. These findings provide initial evidence of the critical role that the SPACA6P-AS-miR-339-5p/FAM167A axis may play in CRC, suggesting novel avenues for targeted therapy and potential biomarkers for this disease.

## 2 | Materials And Methods

### 2.1 | Bioinformatics Analysis

We first utilized online tools to screen for lncRNAs with the aim of identifying key lncRNAs closely associated with colorectal cancer (CRC). During this process, SPACA6P-AS was identified as an important candidate biomarker. Additionally, we identified several other potentially functional lncRNAs in colorectal cancer. Using the UCSC database (<http://genome.ucsc.edu/>; access date: July 24, 2024) [17], we reviewed the expression data of SPACA6P-AS in normal colon tissue, which helped us understand the baseline expression patterns of this lncRNA in healthy tissues. Through the TCGA database (<http://cancergenome.nih.gov/>; access date: July 24, 2024), we obtained RNA-seq data from the TCGA-COAD and TCGA-READ datasets, which included 647 tumor samples and 51 normal samples, as well as miRNA-seq data from 619 tumor samples and 11 normal samples from the same datasets. To ensure the comparability of data across different samples, we standardized the gene expression data in the COAD and READ datasets. We applied a log2 transformation to the raw RNA-seq count data, and then normalized the RNA-seq and miRNA-seq data using the TPM and RPM methods, respectively, to eliminate the influence of sequencing depth and gene length. Batch effect correction was performed using the ComBat method from the SVA R package (3.52.0). Statistical analyses were conducted using the stats (4.2.1) and car (3.1-0) R packages in R software (4.2.1), and differential expression of SPACA6P-AS, miR-339-5p, miR-324-3p, and FAM167A in tumor and normal tissues was visualized using the ggplot2 package (3.3.6). Outliers were detected through scatter plots. Using the lncAR database (<https://lncar.renlab.org/>; access date: July 26, 2024) [18], we obtained differential expression data for SPACA6P-AS from the GEO datasets GSE73360 and GSE90524.

To further investigate other key factors in colorectal cancer, we used the GEPIA database (<http://gepia2.cancer-pku.cn/>; access date: July 24, 2024) [19]. Subsequently, we analyzed the expression levels of FAM167A, miR-339-5p, and miR-324-3p in CRC tissues to further determine their roles in

colorectal cancer progression. Using the starBase 2.0 database (<http://starbase.sysu.edu.cn>; access date: July 24, 2024) [20], we conducted in-depth correlation analyses. In particular, we explored the correlations between FAM167A, SPACA6P-AS, and miR-339-5p in colorectal cancer samples. This helped us understand the potential interactions between these factors and their possible combined roles in cancer progression.

### 2.2 | Collection of Patient Clinical Information and Tissue Sampling

We obtained human colorectal cancer tissues and corresponding adjacent normal tissues from patients undergoing colorectal cancer surgery at the Second Affiliated Hospital of Harbin Medical University. All patients voluntarily participated and signed informed consent forms during the sample collection process. Tissue samples were collected immediately under sterile conditions after surgical resection and were rapidly frozen and stored in an ultra-low temperature freezer at  $-80^{\circ}\text{C}$  to ensure the quality of the samples was not compromised. Strict laboratory procedures were followed during sample handling to prevent contamination and degradation.

**Inclusion Criteria:** All patients were rigorously and synchronously clinically and pathologically diagnosed with colorectal cancer. The inclusion criteria were as follows: (1) Age between 18 and 75 years; (2) No prior anticancer treatments such as radiotherapy, chemotherapy, or targeted therapy before surgery; (3) No history of other malignancies; (4) Normal hematological parameters before surgery, with no severe cardiac, pulmonary, hepatic, or renal dysfunction; (5) Tumor tissues resected during surgery and paired adjacent normal tissues available for experimental analysis.

**Exclusion Criteria:** To maintain the integrity of the tissue samples, patients who had received any form of specific tumor treatment before diagnosis were excluded. The exclusion criteria included: (1) Patients who received anticancer treatment (including chemotherapy, radiotherapy, targeted therapy, etc.) before surgery; (2) Patients with severe cardiac, pulmonary, hepatic, or renal dysfunction; (3) Patients with other malignancies or chronic diseases that could affect prognosis; (4) Tissue samples that did not meet experimental requirements, such as tissue necrosis or insufficient sample quantity; (5) Patients for whom complete follow-up information was not obtained postoperatively or who withdrew from the study midway.

For prognostic analysis purposes, the follow-up period for each patient was precisely calculated, starting from the date of surgery and ending at either the date of death or the last recorded follow-up, whichever was applicable. Informed consent was obtained from each patient before any sample collection, strictly adhering to institutional guidelines to ensure transparency and ethical robustness. The Clinical Research Ethics Committee of the Second Affiliated Hospital of Harbin Medical University granted full approval for this study, ensuring all research activities were conducted within ethical parameters.

### 2.3 | Cell Culture

The LOVO cell line was procured from Beijing BeiNa Chuanglian Biotechnology Research Institute, Beijing, China, while a diverse range of human CRC cell lines including SW1116, SW480, SW620, HCT116, HT29, RKO, and DLD1, alongside the noncancerous colon epithelial cell line, NCM460, were sourced from American Type Culture Collection (ATCC, Manassas, VA, USA). For culture, each cell line was nurtured in a medium supplemented with 10% (v/v) fetal bovine serum (FBS) and maintained in a humidified incubator set at 37°C under a controlled 5% CO<sub>2</sub> environment. Upon reception, cells were immediately assessed for contaminants, then thawed and transferred to culture dishes. Fresh media, fortified with 10% FBS, was introduced to the dishes. Regular media changes and necessary sub-cultures ensured optimal growth conditions and routine inspections confirmed cellular health and contamination-free cultures.

### 2.4 | SPACA6P-AS-shRNA Plasmid and Cell Transfection

The custom-designed shRNA plasmid targeting SPACA6P-AS was meticulously synthesized by Sangon Biotech (Shanghai, China) using specific primer sequences. The sequences for SPACA6P-AS shRNA are as follows: sense strand: 5'-GATCC GTTCAGGATGCATGGTCTGGCTCGAGCCAGCACCATGC ATCCTGAACTTTTGA-3' and antisense strand: 5'-AGCTTC AAAAAGTTCAGGATGCATGGTCTGGCTCGAGCCAGCAC-CATGCATCCTGAACG-3', designed to minimize off-target effects. The sequence for the negative control (NC) shRNA is: sense strand: 5'-GATCC GTGGATATTGTTGCCATCACTCGA GTGATGGCAACAATATCCACTTTTTGA-3' and antisense strand: 5'-AGCTTCAAAAAGTGGATATTGTTGCCATCACT CGAGTGATGGCAACAATATCCACG-3', used to evaluate nonspecific effects.

Cells destined for transfection were seeded in 6-well plates at a density of  $2 \times 10^5$  cells/well. After reaching 70%–80% confluence, Lipofectamine 2000 (Invitrogen, Carlsbad, CA, USA) was utilized to execute the transfection per manufacturer's directives. 24 h posttransfection, the cells were nourished with a complete medium fortified with 500 µg/ml G418 (Invitrogen, Carlsbad, CA, USA) for 2 weeks. After this period, G418 was

removed, and cells were sustained in the complete medium until stable clones emerged.

In this study, we first constructed the SPACA6P-AS overexpression plasmid (OE SPACA6P-AS-3) by amplifying the full-length cDNA sequence of SPACA6P-AS using PCR and cloning it into the pcDNA3.1 vector. The plasmid was then amplified in *Escherichia coli* and purified to obtain high-quality plasmid DNA. Next, SW620 and LOVO cells were seeded into 6-well plates, and when the cell density reached 70%–80%, the OE SPACA6P-AS-3 plasmid was transfected into the cells using Lipofectamine 3000 reagent. After 24 h of transfection, the medium was replaced with complete medium containing 10% fetal bovine serum (FBS), and G418 (400–800 µg/ml) was added to select for 2–3 weeks to establish a stable SPACA6P-AS overexpressing cell line. The experiment was divided into an overexpression group (OE SPACA6P-AS group) and an empty vector control group (Empty Vector group) to evaluate the role of SPACA6P-AS in the proliferation and apoptosis of colorectal cancer cells.

### 2.5 | Rna Isolation and Real-Time PCR Expression Analysis

The TRIzol reagent (Invitrogen, USA) was employed with precision to isolate total RNA from both tissues and cells. Post extraction, the purity and concentration of RNA were determined through measurements using a Nanodrop 2000 spectrophotometer (Thermo Fisher Scientific, Waltham, MA). For the real-time quantitative PCR (qPCR) assessment, 0.8 µg of the reverse-transcribed cDNA served as the template. It was amplified using the SYBR Green reagent (Thermo Fisher Scientific, Waltham, MA) on the Applied Biosystem 7500 qPCR system (Applied Biosystems). To normalize expression levels and ascertain relative abundance, the  $2^{-\Delta\Delta C_t}$  method was used, designating  $\beta$ -actin as the endogenous reference. Primer sequences specifically harnessed for this study can be found in Table 1.

### 2.6 | Assessment of Cellular Proliferation Using the CCK-8 Assay

To investigate cellular proliferation dynamics posttransfection, we employed the CCK-8 assay (Dojindo, Tokyo, Japan) as a

**TABLE 1** | Primers used for quantitative real-time PCR in this study.

Gene	Primer sequence ( 5' to 3' )
SPACA6P-AS	Forward: GGCGGGAAACAGGTAGGAAAAC Reverse: CACTGTTGAAAGCCCAGCACCAT
FAM167A	Forward: GCTCAGGAAGGAAGTACGG Reverse: GCAGGTGTGTTTCGATTTTCAGC
$\beta$ -actin	Forward: CCTGGCACCCAGCACAAT Reverse: GGGCCGGACTCGTCATAC
U6	Forward: TGCGGGTGCTCGCTTCGGCAGC Reverse: CCAGTGCAGGGTCCGAGGT

robust method for monitoring cell viability. HT29 cells, once transfected, were seeded at a density of 5,000 cells/well into 96-well plates. Their proliferation rates were monitored at three specific intervals: 24, 48, and 72 h post-seeding. To execute the assay, each well was supplemented with 10  $\mu$ l of the CCK-8 solution, followed by an incubation period of 1 h at 37°C. The resulting colorimetric changes, indicative of cell viability, were quantified using a microplate reader (Tecan, Switzerland). Absorbance values, representing cell proliferation, were measured at an optical density (OD) of 450 nm.

## 2.7 | Colony Formation Assay for Cellular Proliferative Capacity

To gauge the proliferative capacity of cells, a colony formation assay was conducted. An initial cell count of  $1 \times 10^3$  cells was plated onto a 6-well plate (sourced from Corning, Life Sciences, USA). Each well was supplemented with 2 ml of the designated growth medium containing 10% FBS to foster cell growth. The plate was set aside for 14 days, allowing colonies to form. After this incubation, cells were fixed using 4% paraformaldehyde for 15 min at room temperature. After a brief wash with PBS, colonies were vividly stained with 0.1% crystal violet for another 15 min. Post-staining, the plate was left to dry before photos of the stained colonies were captured. Quantification of the formed colonies was adeptly achieved using ImageJ software.

## 2.8 | Evaluation of Cell Proliferation Through the EdU Incorporation Assay

To assess cell proliferation, treated cells were initially re-suspended in a 24-well plate. EdU was then added to the culture medium as a marker for actively dividing cells. Following a 2-h incubation period for EdU incorporation, the cells underwent fixation with a 4% paraformaldehyde solution. Excessive paraformaldehyde was subsequently neutralized using glycine. After a thorough rinse with PBS, the cells were treated with Apollo staining solution (acquired from RiboBio, Guangzhou, China) without light. A room-temperature incubation for 30 min was facilitated using a decolorization shaker. For cell permeabilization, a permeate solution was introduced and subjected to a 20-min shaking on the decolorization shaker. For visualization of cell nuclei, Hoechst 33342 was applied, followed by a 30-min incubation in the dark on the shaker.

## 2.9 | Establishing Xenograft Tumors in BALB/c Nude Mice

BALB/c nude mice, aged 4–6 weeks, were housed under strict, specific, pathogen-free conditions, adhering to protocols approved by the Animal Care and Use Committee. To initiate the xenograft tumor model,  $1 \times 10^7$  SW620 Sh-NC and Sh-SPACA6P-AS cells were subcutaneously administered to the mice, with five mice designated for each cell type. For 22 days, the growing tumor volume was periodically measured every 3 days. Measurement was done using a caliper, and the tumor volume was computed based on the formula  $(A \times B^2)/2$ , where

‘A’ represents the longest diameter and ‘B’ is its perpendicular counterpart. On day 22, the mice were euthanized, and tumors were surgically extracted. Removed tumors were then fixed in 4% paraformaldehyde in preparation for subsequent immunohistochemical analyses. This study strictly adhered to internationally recognized guidelines for the ethical conduct of animal experimentation. All animal experiments were performed under specific pathogen-free conditions and received approval from the Ethics Review Committee of the Second Affiliated Hospital of Harbin Medical University. Throughout all experiments, utmost efforts were made to ensure the welfare of the animals and minimize their suffering.

## 2.10 | SPACA6P-AS Detection Via Fluorescent In Situ Hybridization (FISH)

To detect SPACA6P-AS using fluorescent in situ hybridization, cells were rinsed with a 0.5% Triton X-100 in 1 $\times$  phosphate buffered saline (PBS) solution. Subsequently, they were hybridized overnight at 37°C in a humidified chamber with the anti-SPACA6P-AS oligodeoxy-nucleotide probe (sequence: 5DigN-TGAATGAGGAGGTTCTATAAGCCTAGATATGGGA GGATC-3DigN; RiboBio, Guangzhou, China) prepared in a 1% blocking solution. After this, cells underwent sequential washing at 42°C in the dark: three 5-min washes in 0.1% Tween-20 with 4 $\times$  sodium citrate buffer (SSC), a 5-min wash in 2 $\times$ SSC, and a 5-min wash in 1 $\times$ SSC. It was followed by a room temperature 5-min PBS wash, DAPI staining for nuclei visualization, and three more 5-min washes in 1 $\times$ PBS. Imaging was conducted to observe probe localization.

## 2.11 | Luciferase Reporter Assay for miR-339-5p Binding in SPACA6P-AS and FAM167A 3'-UTRs

For assessing miR-339-5p binding, putative wild-type (wt) and mutant (mut) miR-339-5p-binding sites located in the 3'-UTR of SPACA6P-AS or FAM167A mRNA were cloned. The resulting constructs, termed pmirGLO-SPACA6P-AS-wt/mut and pmirGLO-FAM167A-wt/mut, were integrated into the pmirGLO-Report luciferase vector (sourced from GenePharma, Shanghai, China). miR-339-5p mimics and inhibitors (acquired from RiboBio, Guangzhou, China) were employed to amplify or suppress the miR-339-5p levels. These constructs were transiently transfected into HEK293 cells. 48 h post-transfection, cells were collected and analyzed using the Dual-Luciferase Reporter Assay System (Promega, USA) as per the instructions provided by the manufacturer.

## 2.12 | Western Blot

Proteins were first separated using 10% SDS-PAGE and transferred onto PVDF membranes. To block nonspecific binding, membranes were incubated in a blocking buffer for 90 min at room temperature. Following this, membranes were probed with primary antibodies against FAM167A (1:1000 dilution, NBP1-91236, NOVUS, USA) and GAPDH (1:1000 dilution, NB300-221, NOVUS, USA) as an internal control, overnight at

4°C. After washing to remove unbound antibodies, membranes were incubated with horseradish peroxidase (HRP)-conjugated secondary antibody to detect the primary antibodies. The bound secondary antibody was visualized using enhanced chemiluminescence, and the emitted light was captured on chemiluminescent film. The ImageLab software was then employed to quantify the band intensities for protein expression levels.

### 3 | Immunohistochemical (IHC) Analysis

For the IHC analysis, paraffin-embedded patient tissues were prepared as per the methodology outlined in previous studies. In detail, tissue samples were embedded in paraffin blocks and subsequently sectioned into thin slices ranging from 2- to 4-μm thick. Following deparaffinization and rehydration, the tissue sections underwent antigen retrieval. Antibodies targeting FAM167A were applied for IHC staining, strictly adhering to the manufacturer's recommended protocol. After completing the staining process, the sections were visualized and imaged using a high-resolution digital microscope camera.

#### 3.1 | Statistical Analyses

To ensure the accuracy and significance of our data, a range of statistical methodologies were employed in this study. For comparisons of means between two groups, we used the Student's t-test; when the two groups did not follow a normal distribution, we applied the non-parametric Wilcoxon rank sum test. For categorical data, we utilized the chi-square test. Survival data were presented using the Kaplan-Meier curves, and differences between survival curves of different groups were assessed using the log-rank test. All data are expressed as the mean ± standard deviation (SD). Throughout our study, probability values (*p*-values) less than 0.05 were considered statistically significant.

## 4 | Results

### 4.1 | Elevated Expression of SPACA6P-AS in Colorectal Cancer

We utilized multiple online bioinformatics tools aiming to identify lncRNAs potentially involved in the initiation and progression of CRC. From the UCSC database, we found that SPACA6P-AS is expressed across all tissue types (Figure 1A). We analyzed transcriptomic sequencing data from the TCGA COAD and READ datasets, including 647 tumor and 51 normal samples. Notably, SPACA6P-AS expression was significantly upregulated in colorectal tumor tissues (Figure 1B). Differential analysis of the GEO datasets GSE73360 and GSE90524 also revealed that SPACA6P-AS is significantly upregulated in colorectal cancer tissues, and its expression was markedly higher in tissues with advanced tumor stages compared to those with lower stages (Figure S1A–B). Additionally, insights from the GEPIA database showed that although SPACA6P-AS expression was not significantly correlated with overall survival in the READ data set or the combined COAD and READ data set

(Figure S1C–D), patients with high SPACA6P-AS expression in the COAD data set had a lower overall survival rate (Figure 1C).

In line with this, our clinical samples also showcased an increased expression of SPACA6P-AS in tumor tissues compared to their adjacent normal counterparts (Figure 1D). Based on SPACA6P-AS expression levels, patients were stratified into high and low groups (Figure 1E). Kaplan-Meier survival curve analysis coupled with the log-rank test demonstrated that CRC patients with subdued SPACA6P-AS expression possessed a more favorable overall survival (OS) rate as opposed to those with pronounced SPACA6P-AS expression (Figure 1F, *p* = 0.046). These findings underscore the pivotal role of SPACA6P-AS expression in prognosticating CRC outcomes.

### 4.2 | Association of lncRNA SPACA6P-AS Expression With Clinicopathological Features in Colorectal Cancer

In our comprehensive exploration of the molecular landscape of colorectal cancer (CRC), we delved into the role and significance of the long noncoding RNA (lncRNA) SPACA6P-AS. As specific lncRNAs increasingly influence cancer initiation and progression, establishing their associations with clinicopathological parameters could elucidate their potential as diagnostic and prognostic biomarkers.

We rigorously examined its correlation with various clinicopathological characteristics to elucidate the clinical implications of SPACA6P-AS expression in CRC. As detailed in Table 2, notable associations were observed between levels of SPACA6P-AS expression and factors including CEA level (*p* = 0.369), tumor size (for tumors ≥ 5 cm, four instances of high expression vs. 0 of low expression, *p* = 0.116). Additionally, lymph node metastasis (for N0, nine instances of high expression vs. 16 of low expression, *p* = 0.038), tumor depth (for T1 + T2, three instances of high expression vs. 19 of low expression, *p* = 0.000), and differentiation degree of the tumor showed significant correlation with SPACA6P-AS. For moderately/poorly differentiated tumors, there were 11 instances of high expression compared to just one of low expression (*p* = 0.000). It could suggest that elevated SPACA6P-AS expression might be associated with tumor malignancy. Conversely, SPACA6P-AS expression did not demonstrate significant correlations with other parameters, such as age and gender.

In conclusion, our findings underscore the potential of increased SPACA6P-AS expression as a valuable prognostic indicator, possibly shaping the future of diagnosis and prognosis assessment for CRC patients.

### 4.3 | Role of lncRNA SPACA6P-AS in Enhancing the Proliferation of CRC Cells

Our preliminary studies discovered a notable correlation between the overexpression of SPACA6P-AS in colorectal cancer (CRC) and tumor progression. To further delve into its role, we first validated the expression of SPACA6P-AS across various



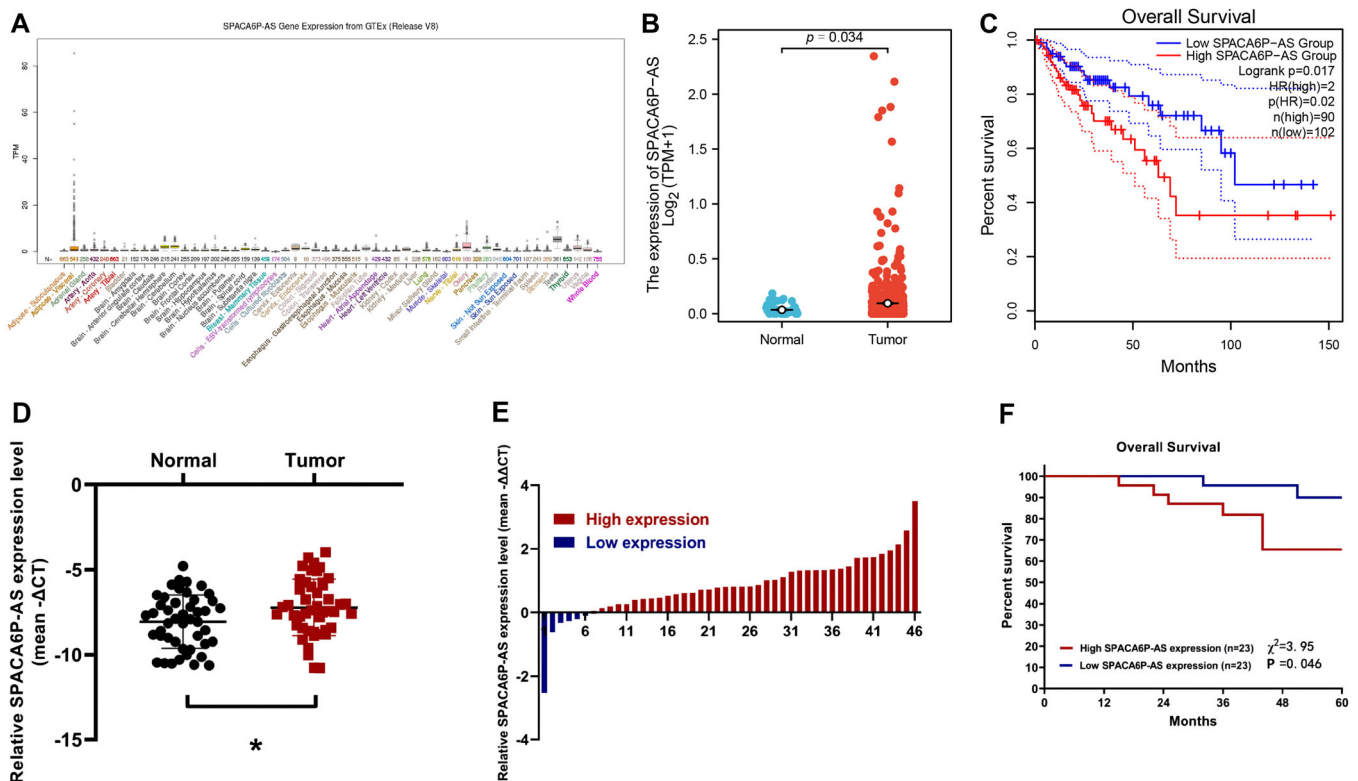


**FIGURE 1** | Expression and prognostic significance of SPACA6P-AS in colorectal cancer (CRC). Note: (A) Expression level of SPACA6P-AS in normal colon tissues (Source: UCSC database). (B) Expression level of SPACA6P-AS in CRC tissues compared to normal tissues (Source: TCGA database, Tumor = 647, Normal = 51). (C) The relationship between SPACA6P-AS expression and overall survival in CRC patients in the COAD data set (Source: TCGA database). (D) Comparison of SPACA6P-AS expression between CRC and adjacent normal tissues ( $n = 46$ ). (E) CRC patients are categorized based on high and low expression of SPACA6P-AS (Low expression = 6, high expression = 40). (F) Kaplan-Meier survival curve showing the relationship between SPACA6P-AS expression and overall survival rate in CRC patients ( $n = 23$ ).

colorectal cancer cell lines and a standard colorectal cell line, namely NCM460, SW480, HCT116, DLD-1, LOVO, HT29, and SW620. Notably, NCM460 serves as a regular colon mucosal epithelial cell line, often representing healthy colorectal cells. SW480, HCT116, DLD-1, LOVO, and HT29 are all derived from human colorectal adenocarcinomas. Intriguingly, SW480 and SW620 are from the same patient, with SW620 isolated from liver metastasis, indicating a more advanced and aggressive CRC stage. Significantly, we observed an elevated expression of SPACA6P-AS in the SW620 and LOVO cell lines, while its expression in SW480 was diminished (Figure 2A). Consequently, SW620 and LOVO were chosen as representatives for subsequent research.

Existing data posits that the upregulation of SPACA6P-AS can be an independent predictor of overall survival in CRC patients. To further dissect the role of SPACA6P-AS in the evolution and progression of CRC, we downregulated its expression in SW620 and LOVO cells using shRNA and utilized G418 to select stably transfected cell lines. By screening sh-SPACA6P-AS in SW620 cells, results highlighted that sh-SPACA6P-AS-3 had the highest silencing efficiency (Figure 2B), making it our choice for further experiments. We selected other genes from the SPACA6 family, including SPACA1, SPACA3, SPACA4, and SPACA5, as controls. Through qPCR analysis, we found that the mRNA and protein expression levels of these genes did not show significant changes in CRC cells transfected with sh-SPACA6P-AS,

indicating that the knockdown effect of sh-SPACA6P-AS is highly specific (Figure 2C). In the SW620 and LOVO cells, compared to the NC shRNA transfected group, the levels of SPACA6P-AS were reduced by  $79.78\% \pm 6.46\%$  and  $70.44\% \pm 6.17\%$ , respectively (Figure 2D), affirming that lncRNA SPACA6P-AS was consistently downregulated in these cell lines. Results from the CCK-8 assays and colony formation tests indicated that the proliferation capacities of transfected CRC cells were significantly hampered compared to the control group (Figure 2E–F). Validating this diminished proliferation, we conducted an EdU assay and apoptosis analysis, which revealed a reduced green fluorescence in the EdU assay when SPACA6P-AS was knocked down (Figure 2G). In summary, our findings underscore that the downregulation of SPACA6P-AS significantly curtails the proliferative abilities of colorectal cancer cells, suggesting its pivotal role in tumor progression.

To further investigate the effects of SPACA6P-AS on CRC cell proliferation and apoptosis, we constructed an SPACA6P-AS overexpression plasmid and transfected it into SW620 and LOVO cells. The qPCR results showed that the mRNA levels of SPACA6P-AS in the overexpression group were significantly higher than those in the control group in both SW620 and LOVO cells (Figure S2A). The CCK-8 proliferation assay indicated that SPACA6P-AS overexpression significantly promoted the proliferation of SW620 and LOVO cells (Figure S2B). Additionally, the

**TABLE 2** | Association between SPACA6P-AS expression and clinicopathological features in colorectal cancer patients.

Characteristics	Total	Expression of SPACA6P-AS		<i>p</i> value
		High ( <i>n</i> = 23)	Low ( <i>n</i> = 23)	
Gender				1.000
Female	22	11	11	
Male	24	12	12	
Age (year)				0.765
≥ 55	19	9	10	
< 55	27	14	13	
Tumor size (cm)				0.116
≥ 5	4	4	0	
< 5	42	19	23	
Differentiation				0.000
Moderate/poor	12	11	1	
Well	34	12	22	
Depth of tumor				0.000
T1 + T2	22	3	19	
T3 + T4	24	20	4	
Lymph node metastasis (N)				0.038
N0	25	9	16	
N1 or above	21	14	7	
CEA level				0.369
Negative	27	12	15	
Positive	19	11	8	

colony formation assay demonstrated a substantial increase in the number of colonies formed by cells overexpressing SPACA6P-AS (Figure S2C). Similarly, to confirm this proliferative capacity, we performed EdU assays and apoptosis analysis. Compared with the control group, the EdU assay showed a marked increase in green fluorescence when SPACA6P-AS was overexpressed (Figure S2D). These findings further demonstrate the critical role of SPACA6P-AS in promoting colorectal cancer cell proliferation and inhibiting apoptosis, supporting its scientific significance as a potential therapeutic target for colorectal cancer.

**4.4 | In Vivo Evidence: Knockdown of lncRNA SPACA6P-AS Impedes Tumor Growth in Colorectal Cancer**

Our preliminary in vitro experiments discovered that SPACA6P-AS plays a pivotal role in the proliferation of colorectal cancer cell lines. Subsequent in vivo studies utilizing a mouse model with SPACA6P-AS knockdown revealed that mice injected with SPACA6P-AS knockdown SW620 cells exhibited smaller tumors than the control group (Figure 3A). Additionally, there was a slight reduction in the weight of these mice compared to the controls (Figure 3B). Detailed tumor measurements further corroborated that tumors from the treated group were notably smaller than those from the control group (Figure 3C). Even post-excision, this observation held, with

tumors from the shRNA-SPACA6P-AS group being significantly smaller than those in the control group (Figure 3D). Pronounced variations were observed in both tumor weight and volume between the two groups (Figure 3E–F). Moreover, tumor tissue immunohistochemistry (IHC) results depicted decreased expression of proliferation markers PCNA and Ki-67 in tumors with diminished lncRNA SPACA6P-AS expression (Figure 3G).

Our findings underscore the potential role of lncRNA SPACA6P-AS in promoting the growth of colorectal cancer tumors. Reducing SPACA6P-AS in SW620 cells not only scaled down the tumor size but also altered the expression of key proliferation markers. These discoveries suggest that SPACA6P-AS may be a viable therapeutic target for colorectal cancer treatment.

**4.5 | lncRNA SPACA6P-AS Directly Interacts With miR-339-5p in CRC**

Long noncoding RNAs (lncRNAs) have garnered attention for their multifaceted roles in various cellular processes, particularly in cancer. Among these lncRNAs, SPACA6P-AS has recently been implicated in colorectal cancer (CRC) progression. This study sought to elucidate the specific interactions of SPACA6P-AS in CRC and its potential mechanism of action.

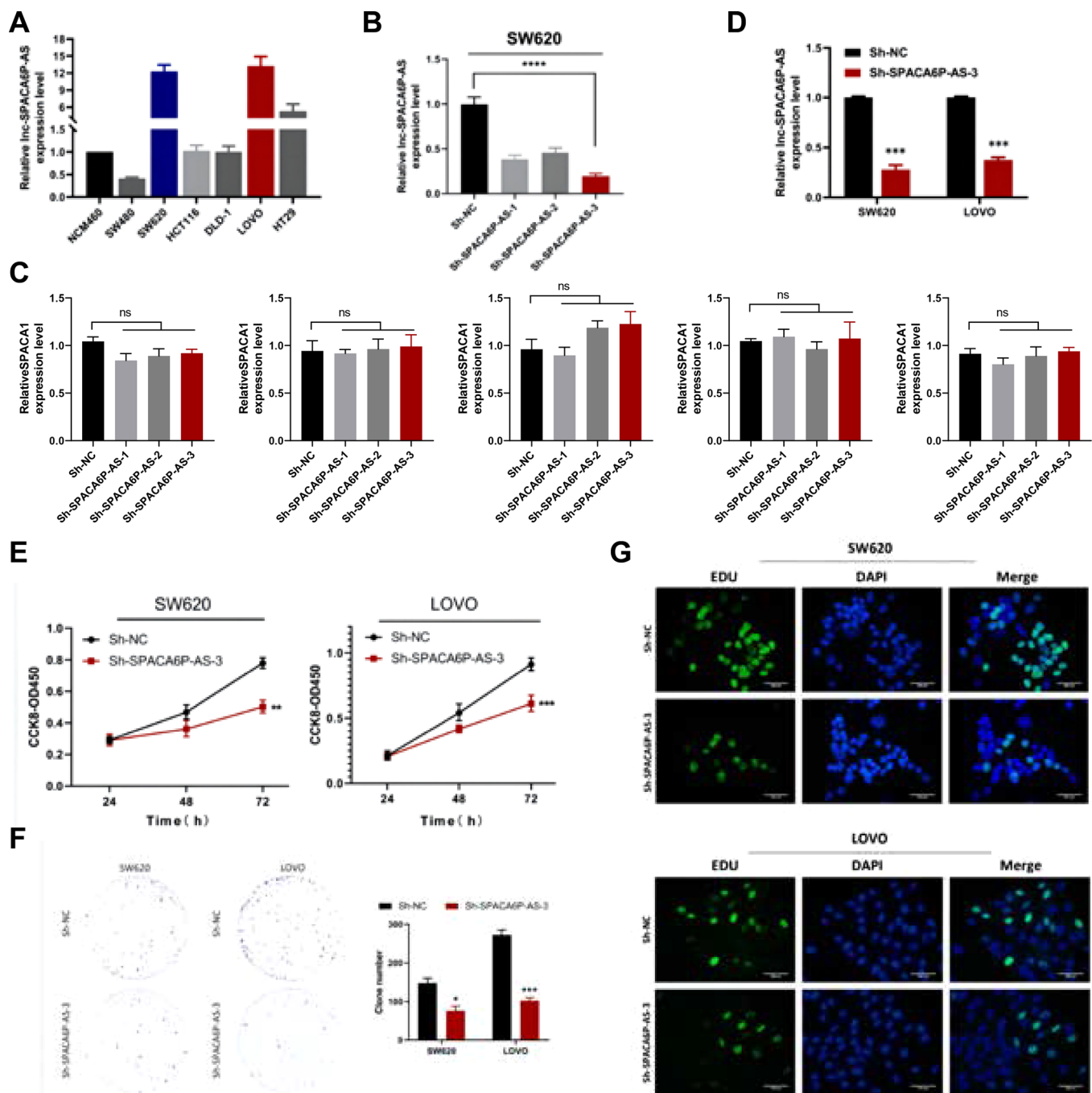


**FIGURE 2** | Effect of SPACA6P-AS on in vitro proliferation of colon cancer cells. Note: (A) Relative expression of SPACA6P-AS in normal and various tumor cell lines ( $n = 3$ ). (B) Efficiency of silencing by sh-SPACA6P-AS-1, sh-SPACA6P-AS-2, and sh-SPACA6P-AS-3 in SW620 cell line ( $n = 3$ ). (C) Validation of the specificity of sh-SPACA6P-AS: mRNA expression levels of SPACA6P-AS and other SPACA6 family genes (SPACA1, SPACA3, SPACA4, and SPACA5) in CRC cells transfected with sh-SPACA6P-AS ( $n = 3$ ). (D) Silencing efficiency of sh-SPACA6P-AS-3 in SW620 and LOVO cell lines ( $n = 3$ ). (E–F) Proliferative capacity of CRC cells after transfection with shSPACA6P-AS-3, assessed by CCK-8 assay and colony formation assay ( $n = 3$ ). (G) Proliferative activity of CRC cells after transfection with shSPACA6P-AS-3, assessed by EdU assay and apoptosis analysis ( $n = 3$ ).

Consistent with prior studies suggesting that the functional role of lncRNA varies based on its cellular localization [21–23], fluorescence in situ hybridization (FISH) results indicated a predominant cytoplasmic localization for SPACA6P-AS (Figure 4A). Given recent discoveries highlighting the ability of certain lncRNAs to act as competitive endogenous RNAs (ceRNAs) for miRNAs, thereby influencing their biological functions [16], we pursued this line of inquiry for SPACA6P-AS.

Utilizing the starBase online software (<http://starbase.sysu.edu.cn>), we identified 10 miRNAs with complementary base pairing potential to SPACA6P-AS, given stringent criteria (scores > 1000). Of these, only miR-339-5p and miR-324-3p displayed aberrant expression patterns in CRC tissues, as evidenced by starBase 2.0 (Figure 4B). qPCR analysis further corroborated the diminished expression of both miRNAs in cancerous compared to normal tissues (Figure 4C). Intriguingly, SPACA6P-AS



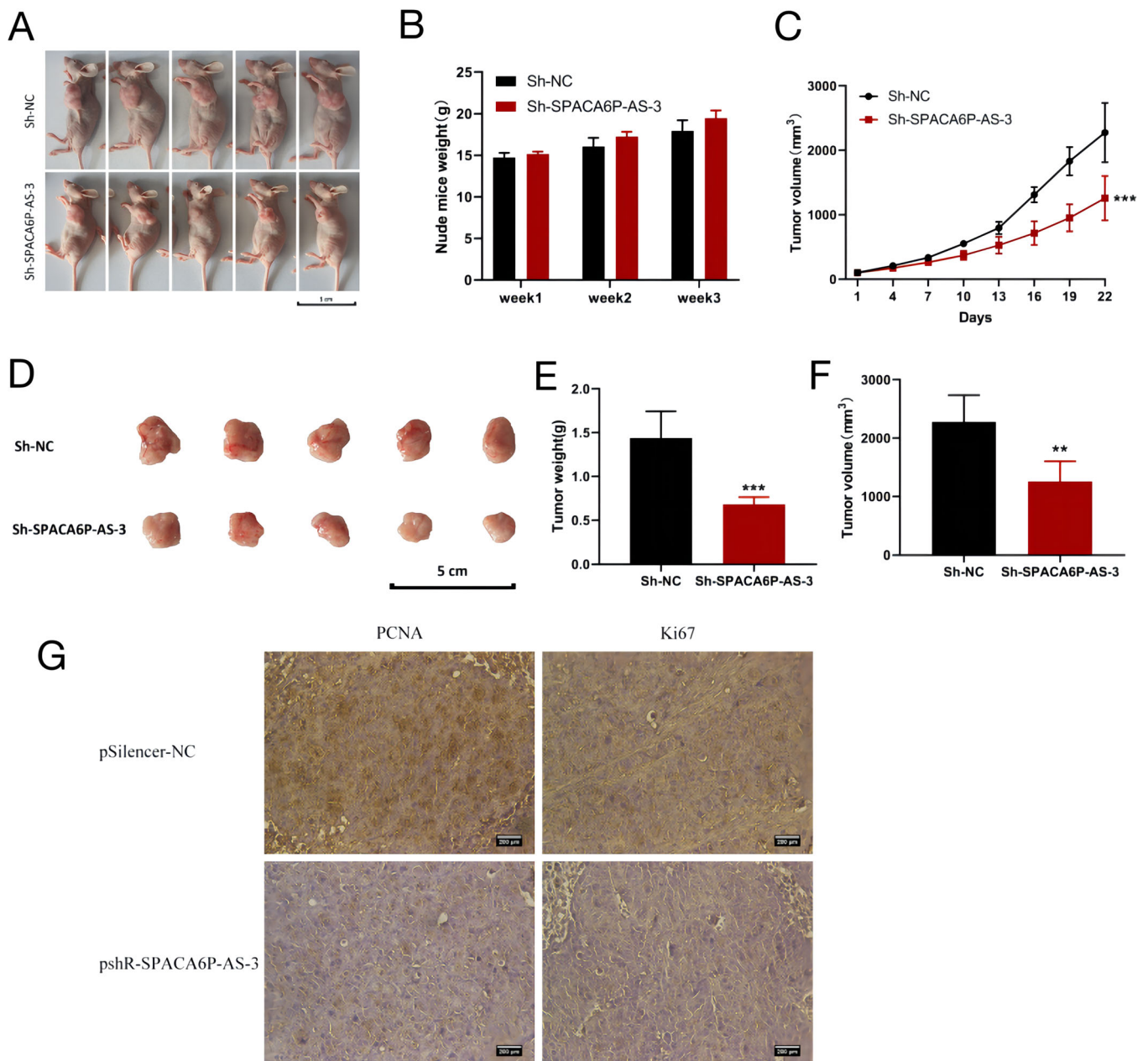


**FIGURE 3** | Comparative tumor growth and marker expression analysis between SPACA6P-AS knockdown mice and control mice. Note: (A) Comparison of tumor sizes in mice. Bottom row: mice injected with SPACA6P-AS knockdown SW620 cells. Top row: control group ( $n = 5$ ). (B) Weight comparison of both groups of mice. Red bars represent mice injected with SPACA6P-AS knockdown SW620 cells. Black bars represent the control group ( $n = 5$ ). (C) Graphical representation of tumor size differences between shSPACA6P-AS group (red) and shNC group (black) ( $n = 5$ ). (D) Photographic evidence of excised tumors. Bottom row: tumors from shSPACA6P-AS knockdown group. Top row: tumors from the shNC group ( $n = 5$ ). (E) Bar chart showing the weights of excised tumors from the two groups. Red bars represent tumors from the shSPACA6P-AS group. Black bars represent the shNC group ( $n = 5$ ). (F) Bar chart showing the volume differences between tumors of the two groups. Red bars represent tumors from the shSPACA6P-AS group. Black bars represent the shNC group ( $n = 5$ ). (G) Immunohistochemistry (IHC) results for proliferative markers PCNA and Ki-67. Bottom row: tumors with reduced expression of shSPACA6P-AS. Top row: tumors from the shNC group ( $n = 5$ ).

expression exhibited a negative correlation solely with miR-339-5p in CRC tissues, while its relationship with miR-324-3p remained nonsignificant (Figure 4D).

To ascertain the direct interaction between SPACA6P-AS and miR-339-5p, we generated luciferase reporter constructs harboring either the wild-type or mutated sequences of SPACA6P-AS (Figure 4E). Overexpression of miR-339-5p distinctly

suppressed the luciferase activity linked to the wild-type SPACA6P-AS, while its inhibition enhanced activity. These effects were absent in the mutant SPACA6P-AS group upon miR-339-5p modulation (Figure 4F).

In conclusion, our findings solidify the position of lncRNA SPACA6P-AS as a critical modulator in CRC progression, potentially through its ceRNA interaction with miR-339-5p.

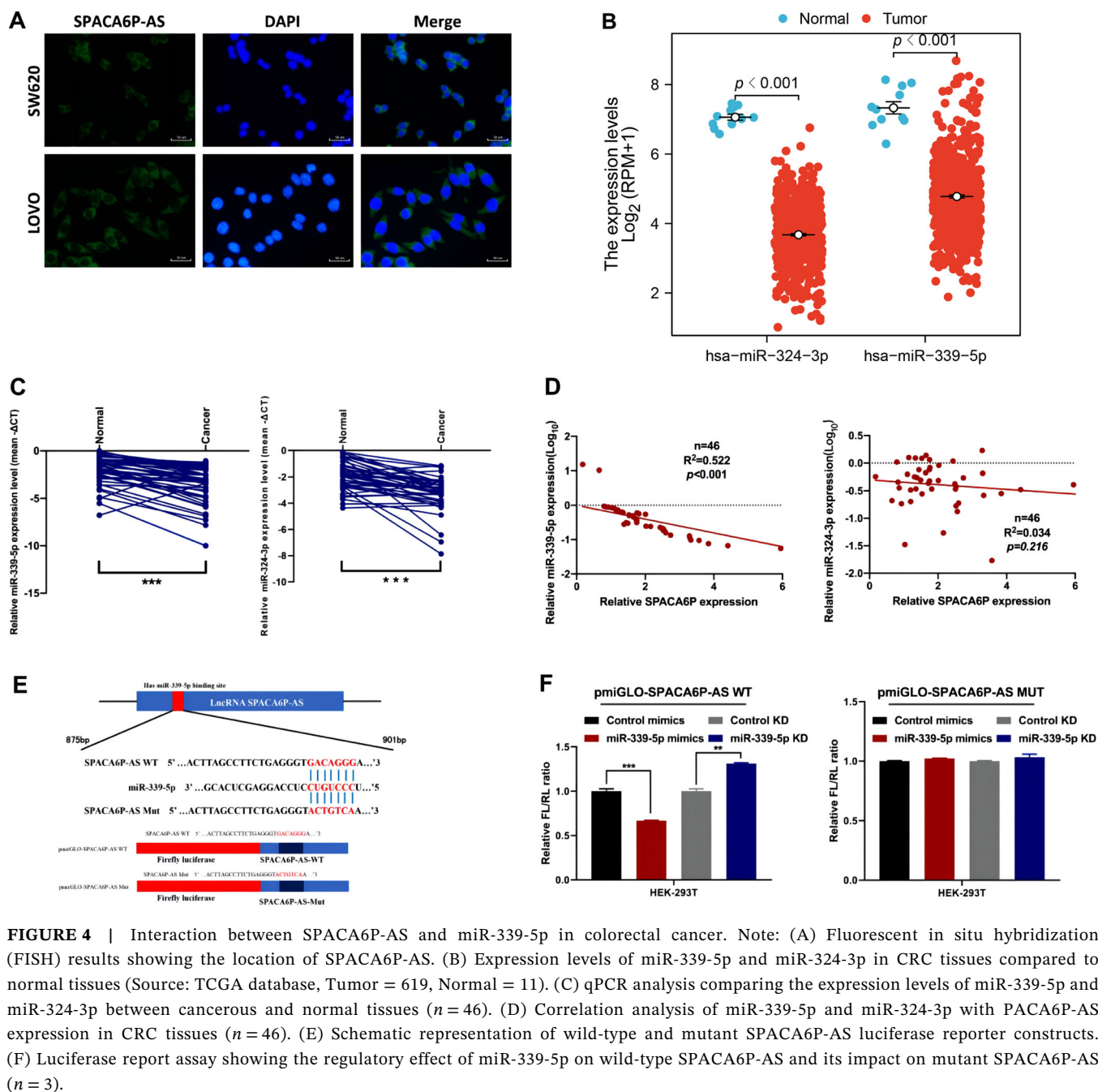


**FIGURE 4** | Interaction between SPACA6P-AS and miR-339-5p in colorectal cancer. Note: (A) Fluorescent in situ hybridization (FISH) results showing the location of SPACA6P-AS. (B) Expression levels of miR-339-5p and miR-324-3p in CRC tissues compared to normal tissues (Source: TCGA database, Tumor = 619, Normal = 11). (C) qPCR analysis comparing the expression levels of miR-339-5p and miR-324-3p between cancerous and normal tissues ( $n = 46$ ). (D) Correlation analysis of miR-339-5p and miR-324-3p with SPACA6P-AS expression in CRC tissues ( $n = 46$ ). (E) Schematic representation of wild-type and mutant SPACA6P-AS luciferase reporter constructs. (F) Luciferase report assay showing the regulatory effect of miR-339-5p on wild-type SPACA6P-AS and its impact on mutant SPACA6P-AS ( $n = 3$ ).

Future therapeutic strategies targeting this interaction could open avenues for novel CRC treatments.

#### 4.6 | LncRNA SPACA6P-AS Regulates CRC Cell Proliferation Through miR-339-5p

Long noncoding RNAs (lncRNAs) have emerged as critical regulators in various cancers, including colorectal cancer (CRC). One such lncRNA, SPACA6P-AS, has gained attention due to its potential oncogenic role in CRC progression. Our previous studies highlighted the potential interaction between SPACA6P-AS and miR-339-5p, prompting us to delve further into their functional relationship in CRC.

We initiated our study based on the hypothesis that SPACA6P-AS might regulate CRC cell growth via miR-339-5p. To validate this, we employed miR-339-5p Antisense Oligonucleotides (ASO) to modulate its expression in CRC cells. As per CCK-8 assays, we found that the decline in cell proliferation triggered by Sh-SPACA6P-AS-3 could be substantially counteracted upon treatment with miR-339-5p ASO (Figure 5A, B). Moreover, a reduced expression of miR-339-5p curbed the degradation capability of CRC cells, which was initially amplified by Sh-SPACA6P-AS-3 (Figure 5C, D). We conducted an EDU experiment to reinforce our findings across three distinct groups. Notably, upon inhibiting miR-339-5p, the proliferative capacity of the cells was reinstated across two different cell lines, aligning with our anticipations (Figure 5E, F).

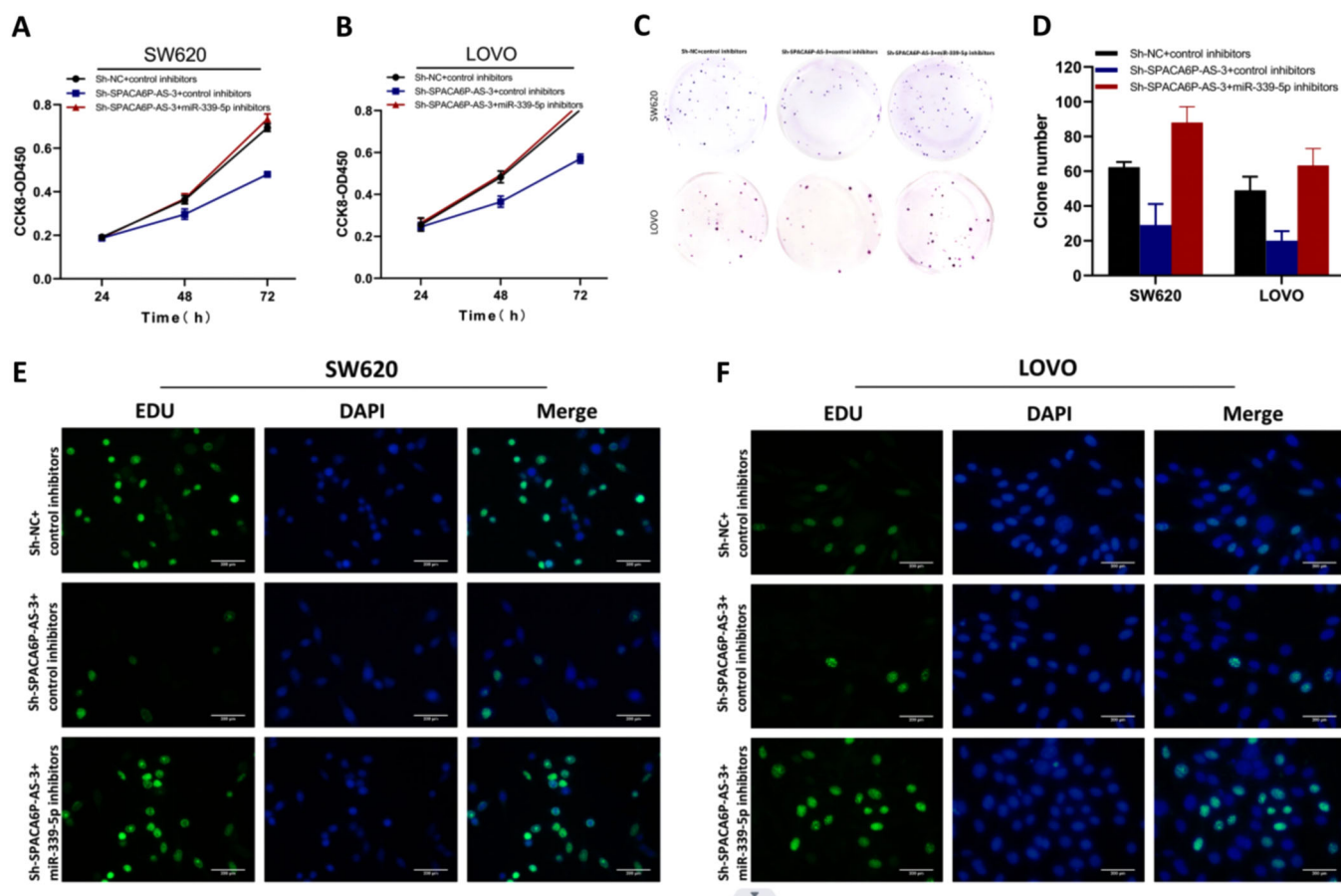


**FIGURE 5** | Functional interaction between lncRNA SPACA6P-AS and miR-339-5p in regulating CRC cell proliferation. Note: (A–B) CCK-8 assay evaluating the proliferative effect of miR-339-5p antisense oligonucleotide (ASO) in SW620 cells (A) and LOVO cells (B) with or without ShSPACA6P-AS-3 transfection ( $n = 3$ ). (C–D) Analysis of the impact of miR-339-5p ASO on cell degradation ability in SW620 cells (C) and LOVO cells (D) with or without ShSPACA6P-AS-3 transfection ( $n = 3$ ). (E–F) Proliferation effect of miR-339-5p ASO in SW620 cells (E) and LOVO cells (F) with or without ShSPACA6P-AS-3 transfection, observed through EdU staining ( $n = 3$ ).

In conclusion, our comprehensive analysis corroborates that SPACA6P-AS drives CRC cell proliferation predominantly through its intricate interaction with miR-339-5p.

#### 4.7 | LncRNA SPACA6P-AS Regulates FAM167A Expression Via Competitive Binding With miR-339-5p

In the intricate interplay of noncoding RNAs in cancer, long noncoding RNAs (lncRNAs) often regulate gene expression via complex interactions with microRNAs (miRNAs). We previously identified the potential role of LncRNA SPACA6P-AS in colorectal cancer (CRC) progression and its interaction with miR-339-5p. Aiming to unveil the downstream regulatory targets, we searched for proteins this interaction might influence.

Our exploratory analysis led us to FAM167A, a protein predicted to be upregulated in colorectal cancer, through online database analysis (Figure 6A). Correlation analyses revealed a positive association between FAM167A and SPACA6P-AS but a negative relationship between FAM167A and miR-339-5p (Figure 6B).

To further validate these associations, we cloned the FAM167A 3' UTR fragment containing either the wild-type or mutant miR-339-5p-binding site downstream of the luciferase open reading frame (Figure 6C). Consistent with our hypothesis, luciferase reporter assays confirmed that the FAM167A 3' UTR is a direct target of miR-339-5p in CRC cells (Figure 6D). Subsequent RT-qPCR and Western blot analyses in SW620 and LOVO cells further demonstrated that the knockdown of SPACA6P-AS downregulates FAM167A expression, a phenomenon which was reversed upon inhibition of miR-339-5p (Figure 6E–H).

In conclusion, our findings elucidate a novel regulatory axis in colorectal cancer, where LncRNA SPACA6P-AS augments FAM167A expression by competitively binding to miR-339-5p.

#### 4.8 | Combined Expression of SPACA6P-AS and FAM167A: A Novel Prognostic Marker for Colorectal Cancer Survival

As research into the mechanisms behind colorectal cancer deepens, novel biomarkers continue to emerge. Survival data from the database illustrated significant disparities between high and low expression cohorts of FAM167 in colorectal cancer (Figure 7A).



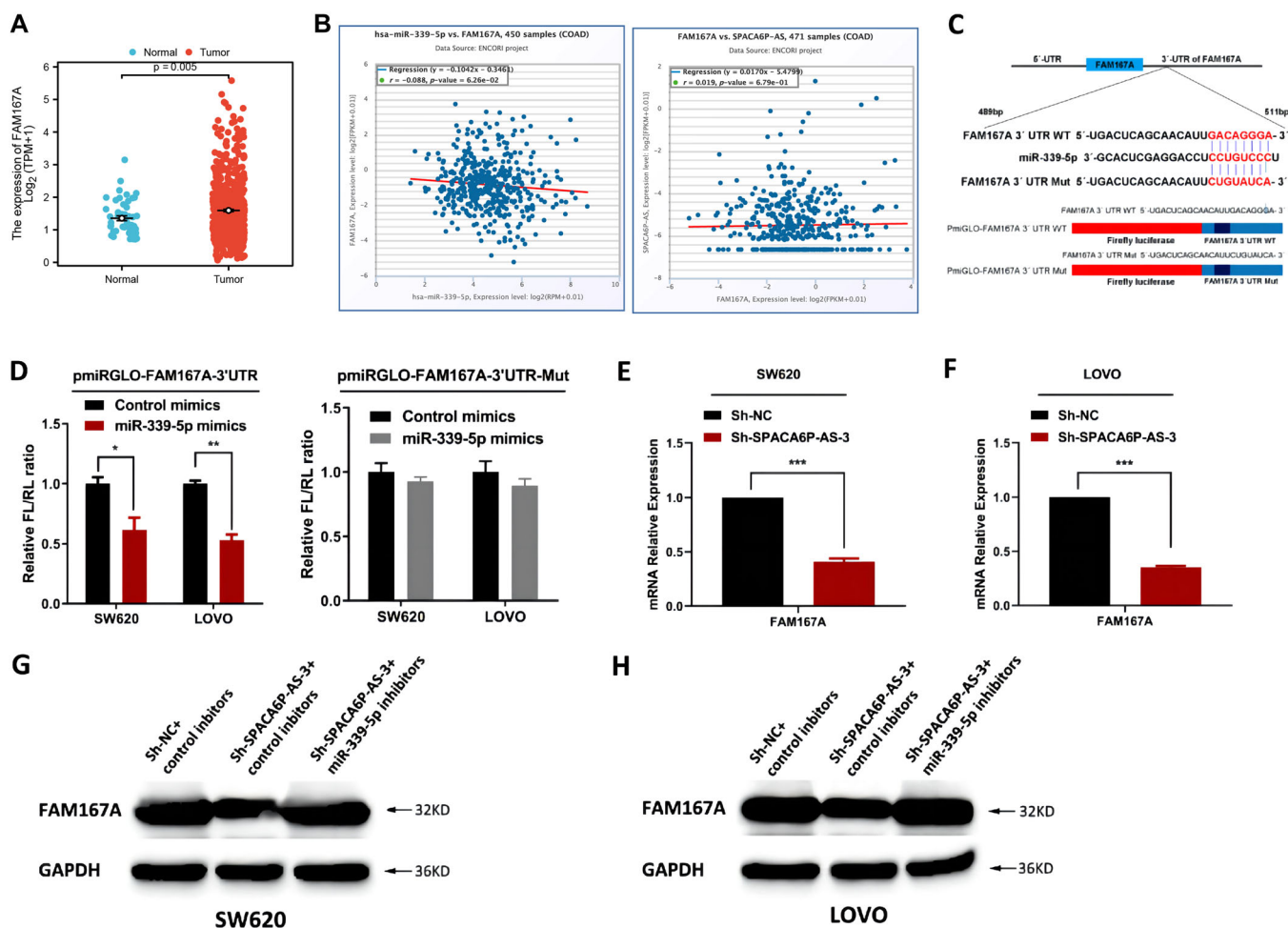


**FIGURE 6** | LncRNA SPACA6P-AS regulates FAM167A expression in colorectal cancer cells by competitively binding with miR-339-5p. Note: (A) Differential expression levels of FAM167A in CRC tissues compared to normal tissues (Source: TCGA database, Tumor = 647, Normal = 51). (B) Correlation analysis of FAM167A with SPACA6P-AS and miR-339-5p in CRC samples using the starBase 2.0 database. (C) Schematic representation of the wild-type and mutant binding sites of miR-339-5p with the 3'UTR of FAM167A. (D) Luciferase reporter assay validating the direct interaction between miR-339-5p and the 3'UTR of FAM167A ( $n = 3$ ). (E-F) RT-qPCR analysis showing the effect of SPACA6P-AS knockdown on FAM167A expression in SW620 and LOVO cells ( $n = 3$ ). (G-H) Western blot analysis showing the effect of miR-339-5p inhibition on FAM167A protein levels in SPACA6P-AS knockdown SW620 and LOVO cells ( $n = 3$ ).

To validate this observation, we sought to corroborate using our in-house data. Patient pathology samples were subjected to immunohistochemical staining, revealing a heightened expression of SPACA6P-AS consistent with FAM167A (Figure 7B). Echoing the preliminary database findings, a positive correlation was discerned between SPACA6P-AS and FAM167A (Figure 7C). We then juxtaposed high and low expression profiles of both SPACA6P-AS and FAM167A to project patient survival outcomes. The findings were telling: pronounced survival rate discrepancies were evident between cohorts with high expressions of SPACA6P-AS and FAM167A and those with diminished expressions of the same (Figure 7D). It offers a novel perspective, positioning the combined expression of SPACA6P-AS and FAM167A as a potential new prognostic marker for colorectal cancer survival.

## 5 | Discussion

Emerging evidence highlights that (lncRNAs are pivotal players in the onset and progression of various cancers [24–26]. In liver

cancer, for instance, the regulatory role of SPACA6P-AS, achieved through competitive binding with miR-125a, has been thoroughly explored [16]. Recent studies have also demonstrated that targeting specific molecular pathways can profoundly influence the progression and therapeutic response of colorectal cancer [27, 28]. However, the function of SPACA6P-AS in CRC remains largely unexplored. This study aims to address this gap in knowledge.

The intriguing study by Xu M and colleagues [29] has revealed that a group of seven lncRNAs, including SPACA6P-AS, correlates significantly with the survival outcomes of breast cancer patients. This finding triggered our interest in examining the role of SPACA6P-AS within the context of gastrointestinal cancers. Our preliminary investigations showed that SPACA6P-AS is typically expressed at low levels in normal tissues such as the colon, liver, and bone marrow. Contrastingly, our data indicates a substantial overexpression of SPACA6P-AS in CRC tissues, implying a potential role in the pathogenesis and

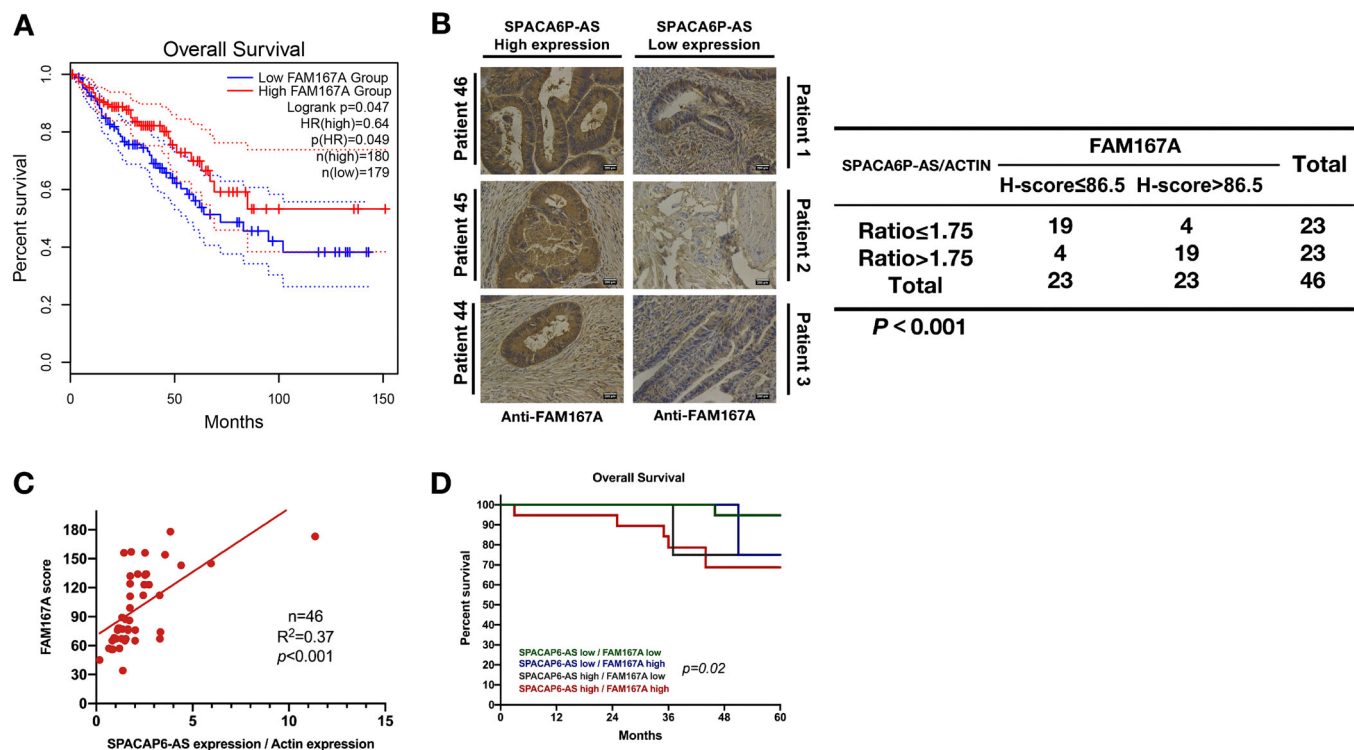


**FIGURE 7** | Association between SPACA6P-AS and FAM167A expression and survival rate in colorectal cancer patients. Note: (A) Survival differences between high and low expression groups of FAM167 in CRC patients from the GEPIA database. (B) Immunohistochemical staining of patient pathological samples showing the expression relationship between SPACA6P-AS and FAM167A ( $n=46$ ). (C) Correlation analysis of SPACA6P-AS and FAM167A expression in colorectal cancer ( $n=3$ ). (D) Comparison of patient survival rates based on combined.

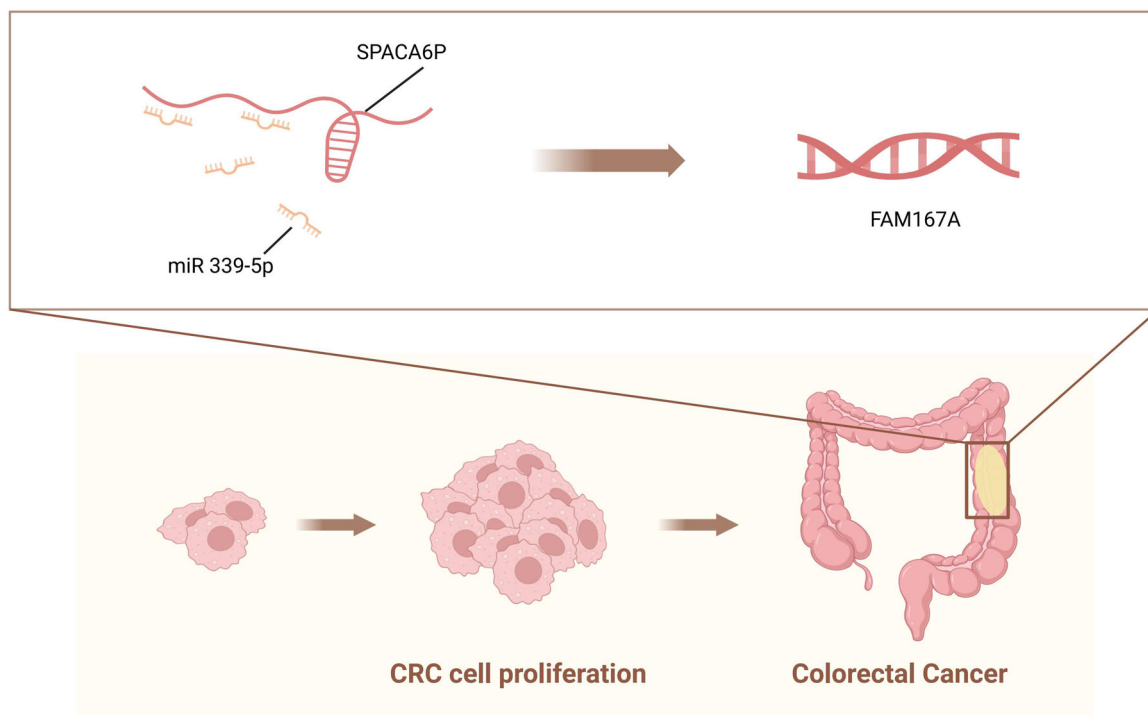


**FIGURE 8** | Schematic representation of the SPACA6P-AS/miR-339-5p/FAM167A axis in colorectal cancer progression.

progression of CRC. Further analyses drew a clear connection between high levels of SPACA6P-AS and reduced survival rates in CRC patients, as evidenced by our evaluations in both CRC cell lines and clinical samples.

## 6 | Conclusion

Our study stands out as the inaugural comprehensive exploration of the functional mechanism of SPACA6P-AS in CRC.



While previous reports have indicated a relatively low expression of this lncRNA in various cancers, our findings contrast these observations, showing a notable upregulation in CRC. This increase in SPACA6P-AS levels is significantly correlated with poorer prognosis in CRC patients, suggesting a different pattern of expression and a possibly unique functional role of SPACA6P-AS in this type of cancer.

To delve deeper into the potential impact of SPACA6P-AS in CRC, we embarked on a series of functional experiments. These studies indicate that the downregulation of SPACA6P-AS is associated with a decrease in the proliferation of CRC cells. This aligns with existing literature suggesting that lncRNAs can act as molecular “sponges,” sequestering miRNAs and thereby influencing the expression of downstream target proteins [30–33]. In the case of SPACA6P-AS, we observed a cytoplasmic localization, which led us to hypothesize a similar sponge-like mechanism in CRC cell proliferation. Through rigorous experimentation and database analysis, we confirmed that SPACA6P-AS indeed regulates the expression of FAM167A by competitively binding with miR-339-5p. This interaction significantly influences CRC cell proliferation, with SPACA6P-AS functioning as a competitive endogenous RNA (ceRNA), thus modulating the miR-339-5p/FAM167A signaling pathway. This mechanism of action of SPACA6P-AS is notably distinct and not commonly observed among other cancer-related lncRNAs.

While our research contributes novel insights into the role of SPACA6P-AS in CRC, it is important to acknowledge the limitations of our study, including the sample size and population diversity. Future studies are needed to further elucidate the molecular mechanisms underlying the function of SPACA6P-AS in CRC and its potential roles in other cancer types. In summary, our findings highlight the crucial role of lncRNA SPACA6P-AS in CRC, particularly its regulatory influence on cell proliferation via the miR-339-5p/FAM167A axis, offering new avenues for therapeutic intervention strategies. Figure 8 provides a schematic representation of the SPACA6P-AS/miR-339-5p/FAM167A axis in colorectal cancer progression, illustrating the complex interplay between these molecular components and their impact on CRC cell proliferation and survival.

#### Author Contributions

**Tianyi Ma:** Conceptualization; Investigation; Funding acquisition; Writing—original draft; Writing—review and editing; Visualization; Software; Data curation. **Yinghu Jin:** Conceptualization; Methodology; Formal analysis; Writing—review and editing; Writing—original draft; Investigation. **Song Wang:** Resources; Writing—review and editing; Investigation; Conceptualization; Methodology; Validation; Visualization; Formal analysis. **Hanqing Hu:** Conceptualization; Investigation; Funding acquisition; Writing—original draft; Writing—review and editing; Visualization; Methodology; Data curation. **Meng Wang:** Methodology; Validation; Visualization; Writing—review and editing; Writing—original draft; Investigation; Conceptualization. **Guoqing Yan:** Conceptualization; Investigation; Funding acquisition; Writing—original draft; Methodology; Validation; Visualization; Writing—review and editing; Formal analysis; Data curation. **Qingchao Tang:** Conceptualization; Methodology; Validation; Formal analysis; Software; Resources; Data curation; Writing—review and editing. **Rui Huang:** Conceptualization; Software; Resources; Data curation; Formal analysis;

Visualization; Validation; Methodology; Writing—review and editing. **Guiyu Wang:** Conceptualization; Investigation; Methodology; Validation; Visualization; Formal analysis; Software; Resources; Writing—review and editing; Project administration; Supervision.

#### Acknowledgments

This research was partially funded by the Scientific Research Project of the Heilongjiang Provincial Health and Family Planning Commission (Grant No. 2018249), the Heilongjiang Provincial Higher Education Innovation Fund (Grant No. 31041210019), and the Second Affiliated Hospital of Harbin Medical University standardized training project for resident doctors (Grant No.2020020225).

#### Conflicts of Interest

The authors declare no conflicts of interest.

#### Ethics Statement

The Clinical Research Ethics Committee of the Second Affiliated Hospital of Harbin Medical University granted full approval for this study, ensuring all research activities fell within ethical boundaries. All animal experiments were performed under specific pathogen-free conditions and received approval from the Ethics Review Committee of the Second Affiliated Hospital of Harbin Medical University. Throughout all experiments, utmost efforts were made to ensure the welfare of the animals and minimize their suffering.

#### Data Availability Statement

The data that support the findings of this study are available from the corresponding author upon reasonable request. To enhance transparency and reproducibility, the raw data underpinning the conclusions presented in this manuscript will be shared openly by the authors upon reasonable request, without any unnecessary restrictions.

#### References

1. R. L. Siegel, K. D. Miller, H. E. Fuchs, and A. Jemal, “Cancer Statistics, 2021,” *Journal of the American Cancer Society* 714 (2021): 7–33, <https://doi.org/10.3322/caac.21654>.
2. S. Mo, W. Dai, H. Wang, et al., “Early Detection and Prognosis Prediction for Colorectal Cancer By Circulating Tumour DNA Methylation Haplotypes: A Multicentre Cohort Study,” *EClinicalMedicine* 55 (2023): 101717, <https://doi.org/10.1016/j.eclinm.2022.101717>.
3. S. de Mey, H. Jiang, H. Wang, et al., “Potential of Memory T Cells in Bridging Preoperative Chemoradiation and Immunotherapy in Rectal Cancer,” *Radiotherapy and Oncology* 127, no. 3 (2018): 361–369, <https://doi.org/10.1016/j.radonc.2018.04.003>.
4. E. Kapiteijn and C. J. H. van De Velde, “European Trials With Total Mesorectal Excision,” *Seminars in Surgical Oncology* 19, no. 4 (2000): 350–357, <https://doi.org/10.1002/ssu.5>.
5. S. Aguiar Junior, M. M. Oliveira, D. R. M. E. Silva, C. A. L. Mello, V. F. Calsavara, and M. P. Curado, “Survival of Patients With Colorectal Cancer in a Cancer Center,” *Arquivos de Gastroenterologia* 57 (2020): 172–177, <https://doi.org/10.1590/S0004-2803.202000000-65>.
6. R. Wang, W. Dai, J. Gong, et al., “Development of a Novel Combined Nomogram Model Integrating Deep Learning-Pathomics, Radiomics and Immunoscore to Predict Postoperative Outcome of Colorectal Cancer Lung Metastasis Patients,” *Journal of Hematology & Oncology* 15, no. 1 (2022): 11, <https://doi.org/10.1186/s13045-022-01225-3>.
7. K. G. Lim, C. S. Lee, D. H. J. Chin, et al., “Clinical Characteristics and Predictors of 5-Year Survival Among Colorectal Cancer Patients in a Tertiary Hospital in Malaysia,” *Journal of Gastrointestinal Oncology* 11, no. 2 (2020): 250–259, <https://doi.org/10.21037/jgo.2020.02.04>.

8. Y. Wang, J. Zhai, X. Wu, et al., "LncRNA Functional Annotation With Improved False Discovery Rate Achieved By Disease Associations," *Computational and Structural Biotechnology Journal* 20 (2022): 322–332, <https://doi.org/10.1016/j.csbj.2021.12.016>.
9. F. Kopp and J. T. Mendell, "Functional Classification and Experimental Dissection of Long Noncoding RNAs," *Cell* 172, no. 3 (2018): 393–407, <https://doi.org/10.1016/j.cell.2018.01.011>.
10. B. Chen, S. Deng, T. Ge, et al., "Live Cell Imaging and Proteomic Profiling of Endogenous NEAT1 lncRNA By CRISPR/Cas9-Mediated Knock-In," *Protein & Cell* 11, no. 9 (2020): 641–660, <https://doi.org/10.1007/s13238-020-00706-w>.
11. E. K. Robinson, S. Covarrubias, and S. Carpenter, "The How and Why of lncRNA Function: An Innate Immune Perspective," *Biochimica et Biophysica Acta (BBA) - Gene Regulatory Mechanisms* 1863, no. 4 (2020): 194419, <https://doi.org/10.1016/j.bbagr.2019.194419>.
12. Z. Yang, S. Jiang, J. Shang, et al., "LncRNA: Shedding Light on Mechanisms and Opportunities in Fibrosis and Aging," *Ageing Research Reviews* 52 (2019): 17–31, <https://doi.org/10.1016/j.arr.2019.04.001>.
13. J. L. Rinn and H. Y. Chang, "Genome Regulation By Long Non-coding RNAs," *Annual Review of Biochemistry* 81 (2012): 145–166, <https://doi.org/10.1146/annurev-biochem-051410-092902>.
14. J. J. Quinn and H. Y. Chang, "Unique Features of Long Non-Coding RNA Biogenesis and Function," *Nature Reviews Genetics* 17, no. 1 (2016): 47–62, <https://doi.org/10.1038/nrg.2015.10>.
15. P. Johnsson, C. Ziegenhain, L. Hartmanis, et al., "Transcriptional Kinetics and Molecular Functions of Long Noncoding RNAs," *Nature Genetics* 54, no. 3 (2022): 306–317, <https://doi.org/10.1038/s41588-022-01014-1>.
16. A. Di Palo, C. Siniscalchi, N. Mosca, A. Russo, and N. Potenza, "A Novel ceRNA Regulatory Network Involving the Long Non-Coding Antisense RNA SPACA6P-AS, miR-125a and Its mRNA Targets in Hepatocarcinoma Cells," *International Journal of Molecular Sciences* 21, no. 14 (2020): 5068, <https://doi.org/10.3390/ijms21145068>.
17. L. R. Nassar, G. P. Barber, A. Benet-Pagès, et al., "The UCSC Genome Browser Database: 2023 Update," *Nucleic Acids Research* 51, no. D1 (2023): D1188–D1195, <https://doi.org/10.1093/nar/gkac1072>.
18. Y. Zheng, Q. Xu, M. Liu, et al., "InCAR: A Comprehensive Resource for lncRNAs From Cancer Arrays," *Cancer Research* 79, no. 8 (2019): 2076–2083, <https://doi.org/10.1158/0008-5472.CAN-18-2169>.
19. C. Li, Z. Tang, W. Zhang, Z. Ye, and F. Liu, "GEPIA2021: Integrating Multiple Deconvolution-Based Analysis Into GEPIA," *Nucleic Acids Research* 49, no. W1 (2021): W242–W246, <https://doi.org/10.1093/nar/gkab418>.
20. J. H. Li, S. Liu, H. Zhou, L. H. Qu, and J. H. Yang, "starBase v2.0: Decoding miRNA-ceRNA, miRNA-ncRNA and Protein-RNA Interaction Networks From Large-Scale CLIP-Seq Data," *Nucleic Acids Research* 42, no. D1 (2014): D92–D97, <https://doi.org/10.1093/nar/gkt1248>.
21. L. Statello, C. J. Guo, L. L. Chen, and M. Huarte, "Gene Regulation By Long Non-coding RNAs and Its Biological Functions," *Nature Reviews Molecular Cell Biology* 22 (2021): 159, <https://doi.org/10.1038/s41580-021-00330-4>.
22. N. Romero-Barrios, M. F. Legascue, M. Benhamed, F. Ariel, and M. Crespi, "Splicing Regulation By Long Noncoding RNAs," *Nucleic Acids Research* 46, no. 5 (2018): 2169–2184, <https://doi.org/10.1093/nar/gky095>.
23. M. Schlackow, T. Nojima, T. Gomes, A. Dhir, M. Carmo-Fonseca, and N. J. Proudfoot, "Distinctive Patterns of Transcription and RNA Processing for Human lincRNAs," *Molecular Cell* 65, no. 1 (2017): 25–38, <https://doi.org/10.1016/j.molcel.2016.11.029>.
24. E. G. Park, S. J. Pyo, Y. Cui, S. H. Yoon, and J. W. Nam, "Tumor Immune Microenvironment lncRNAs," *Briefings in Bioinformatics* 23, no. 1 (2022): bbab504, <https://doi.org/10.1093/bib/bbab504>.
25. J. Yang, F. Liu, Y. Wang, L. Qu, and A. Lin, "LncRNAs in Tumor Metabolic Reprogramming and Immune Microenvironment Remodeling," *Cancer Letters* 543 (2022): 215798, <https://doi.org/10.1016/j.canlet.2022.215798>.
26. Q. P. Liu, J. Y. Lin, P. An, Y. Y. Chen, X. Luan, and H. Zhang, "LncRNAs in Tumor Microenvironment: The Potential Target for Cancer Treatment With Natural Compounds and Chemical Drugs," *Biochemical Pharmacology* 193 (2021): 114802, <https://doi.org/10.1016/j.bcp.2021.114802>.
27. A. Ghasemian, H. A. Omeare, Y. Mansoori, et al., "Long Non-Coding RNAs and JAK/STAT Signaling Pathway Regulation in Colorectal Cancer Development," *Frontiers in Genetics* 14 (2023): 1297093, <https://doi.org/10.3389/fgene.2023.1297093>.
28. J. Liang, W. Dai, C. Liu, et al., "Gingerenone A Attenuates Ulcerative Colitis Via Targeting IL-17RA to Inhibit Inflammation and Restore Intestinal Barrier Function," *Advanced Science (Weinh)* 11, no. 28 (2024): e2400206, <https://doi.org/10.1002/advs.202400206>.
29. M. Xu, Z. Chen, B. Lin, S. Zhang, and J. Qu, "A Seven-lncRNA Signature for Predicting Prognosis in Breast Carcinoma," *Translational Cancer Research* 10, no. 9 (2021): 4033–4046, <https://doi.org/10.21037/tcr-21-747>.
30. Y. Huang, "The Novel Regulatory Role of lncRNA-miRNA-mRNA Axis in Cardiovascular Diseases," *Journal of Cellular and Molecular Medicine* 22, no. 12 (2018): 5768–5775, <https://doi.org/10.1111/jcmm.13866>.
31. H. Luo, C. Xu, W. Le, B. Ge, and T. Wang, "lncRNA CASC11 Promotes Cancer Cell Proliferation in Bladder Cancer Through miRNA-150," *Journal of Cellular Biochemistry* 120, no. 8 (2019): 13487–13493, <https://doi.org/10.1002/jcb.28622>.
32. J. Venkatesh, M. C. D. Wasson, J. M. Brown, W. Fernando, and P. Marcato, "lncRNA-miRNA Axes in Breast Cancer: Novel Points of Interaction for Strategic Attack," *Cancer Letters* 509 (2021): 81–88, <https://doi.org/10.1016/j.canlet.2021.04.002>.
33. X. Kong, Y. Duan, Y. Sang, et al., "lncRNA-CDC6 Promotes Breast Cancer Progression and function as ceRNA to Target CDC6 By Sponging MicroRNA-215," *Journal of Cellular Physiology* 234, no. 6 (2019): 9105–9117, <https://doi.org/10.1002/jcp.27587>.

## Supporting Information

Additional supporting information can be found online in the Supporting Information section.